

Surface Polymerization from Planar Surfaces by Atom Transfer Radical Polymerization Using Polyelectrolytic Macroinitiators

Steve Edmondson,* Cong-Duan Vo, and Steven P. Armes*

Dainton Building, Department of Chemistry, The University of Sheffield, Brook Hill, Sheffield S3 7HF, UK

Gian-Franco Unali

Unilever Research and Development, Port Sunlight, Quarry Road East, Bebington, Wirral, Merseyside L63 3JW, UK

Received April 13, 2007; Revised Manuscript Received May 15, 2007

ABSTRACT: The one-pot synthesis of a new anionic polyelectrolytic macroinitiator based on esterification of a poly(glycerol monomethacrylate) precursor is described. Electrostatic adsorption of this macroinitiator onto an aminated (cationic) planar substrate is monitored by dual polarization interferometry. Controlled surface-initiated polymerization of five hydrophilic methacrylic monomers from this macroinitiator adsorbed onto aminated silicon wafer surfaces is achieved by atom transfer radical polymerization (ATRP) in protic media. The thickness, uniformity, and hydrophilicity of the resulting polymer brushes are characterized by ellipsometry, atomic force microscopy and contact angle studies, and the hydrophilic surface polymerization kinetics is modeled. Microcontact printing is used to produce patterned surfaces with micrometer-sized features. In summary, polyelectrolytic macroinitiators allow the facile synthesis of well-defined polymer brushes on commercially relevant metal oxide surfaces.

Introduction

Densely grafted polymer chains on surfaces (“polymer brushes”)¹ have potential applications in many emerging areas of nanoscience. For example, polymer brushes on nanoparticles² have been used for controlling colloidal stability,^{3–5} for improving matrix compatibility in nanocomposite fabrication,⁶ and for controlling particle self-assembly,⁷ while brush-coated porous substrates can be used as highly selective membranes.^{8,9} Brush-coated planar surfaces have attracted particular interest. The ability to produce stimulus-responsive films^{10–15} has led to suggested applications in sensing^{16–18} and nanoactuation.¹⁹ The robust and solvent-stable nature of brush films has been exploited for lubrication^{20,21} and in antibacterial coatings,²² whereas dense grafting of hydrophilic polymer chains can produce nonfouling surfaces that display remarkable resistance to protein adsorption.²³ Precise control over the thickness and lateral patterning of brush films has been exploited for the fabrication of well-defined quasi-2D objects^{24,25} and also for controlling the assembly of nanoparticles.^{26,27}

Surface-initiated polymerization (SIP) is a so-called “grafting from” technique in which polymer chains are grown directly from initiator sites that are either physically or chemically attached to a surface. SIP enables much higher grafting densities to be achieved than “grafting to” techniques, in which preformed end-functionalized polymer chains are either reacted with or physically adsorbed onto a surface. Thus, SIP allows access to the so-called “brush regime” and enables the fabrication of thick grafted films.

Atom transfer radical polymerization (ATRP)^{28–30} has been used in the vast majority of SIP studies to date.³¹ This technique leads to well-controlled film growth under mild conditions, allows the synthesis of block copolymers, and is applicable to

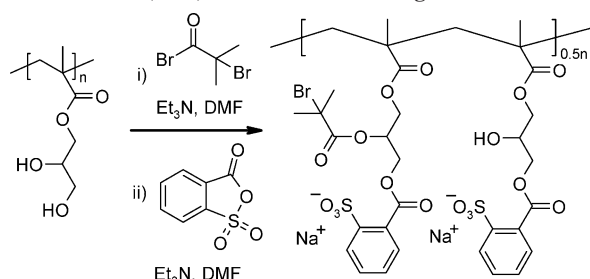
a wide range of functional monomers. Early SIP research focused on planar gold surfaces, which is a convenient model substrate for the chemical grafting of ATRP initiators that also allows surface plasmon resonance³² and electrochemical impedance spectroscopy studies to be conducted.³³ However, gold surfaces suffer from poor long-term chemical stability under oxidative conditions and are simply too expensive for many practical applications. Despite the high activity in this area over the past few years, there remains considerable scope for extending SIP studies to include more common surfaces, such as silica and other metal oxides. Chlorosilane- or alkoxy-silane-based initiators have been typically used for functionalizing oxide surfaces prior to SIP studies.³⁴ Such initiators are generally synthesized by hydrosilylation using highly toxic and flammable reagents (e.g., H_2PtCl_6 and HSiCl_3) and are potentially hazardous with regard to scale-up. This has limited the technological application of SIP, especially for high surface area substrates which require prohibitively large amounts of initiator. Moreover, both types of initiator are prone to hydrolysis, which excludes some potentially interesting colloidal substrates from SIP studies (e.g., waterborne silica sols).

Alternative ATRP initiators for oxide surfaces that avoid hydrosilylation have been reported. However, these reagents either require multiple reaction steps on the surface^{35,36} or involve amide-based initiators¹⁸ which are known to have lower initiator efficiencies than the preferred ester-based initiators.^{37–40}

Both R  he’s group⁴¹ and Luzinov and co-workers⁴² have demonstrated the benefits of using *hydrophobic* macroinitiators on silicon wafers. Recently, Armes and co-workers have reported that polyelectrolytic macroinitiators are interesting alternatives to silane-based and thiol-based ATRP initiators for SIP studies from *colloidal* substrates.^{3,43,44} Such macroinitiators can be conveniently synthesized on a 20–30 g scale, have low toxicity and excellent long-term chemical stability, and can be

* To whom correspondence should be addressed. E-mail: S.Edmondson@sheffield.ac.uk; S.P.Armes@sheffield.ac.uk.

Scheme 1. One-Pot Synthesis of an Anionic Macroinitiator from a Near-Monodisperse PGMA Homopolymer by Sequential Esterification Using First 2-Bromoisobutyryl Bromide (BIBB), Followed by Excess 2-Sulfobenzoic Acid Cyclic Anhydride (SBA) in DMF under Nitrogen^a



^a The final purified anionic macroinitiator had an overall degree of esterification of 82% (~36% hydroxy groups esterified with BIBB and 46% esterified with SBA) as judged by ¹H NMR spectroscopy. The macroinitiator structure shown is approximate, and random esterification of the hydroxy groups on the PGMA chains is expected.

electrostatically adsorbed onto either silica or metal oxide substrates from aqueous solution at ambient temperature. For example, both cationic^{3,43} and anionic⁴⁴ polyelectrolytic macroinitiators have been used to coat several ultrafine aqueous sols (commercial dispersions of either anionic silica, alumina-coated silica, or tin(IV) oxide nanoparticles), and various hydrophilic methacrylic polymers were subsequently grown via ATRP. Advincula's group has also reported some success using an anionic macroinitiator based on poly(acrylic acid) to enable SIP from a latex substrate.⁴⁵

Herein we present the first use of polyelectrolytic macroinitiators for SIP from a model planar substrate (an aminated oxidized silicon wafer). Moreover, we describe the one-pot synthesis of a new anionic macroinitiator derived from poly(glycerol monomethacrylate) (see Scheme 1) that contains a significantly higher proportion of bromoester initiator sites, which ensures that the polymer chains are grown in the brush regime. The adsorbed amount of polyelectrolytic macroinitiator has been determined by dual polarization interferometry, brush thicknesses are calculated from ellipsometric studies, and surface patterning can also be readily achieved. SIP of three hydroxyl-functional methacrylic monomers was investigated in alcohol/water solvent mixtures under various conditions: 2-hydroxyethyl methacrylate (HEMA), glycerol monomethacrylate (GMA), and 2-hydroxypropyl methacrylate (HPMA). Brushes comprising 2-(diethylamino)ethyl methacrylate (DEA) and 2-(diisopropylamino)ethyl methacrylate (DPA) were also grown by ATRP. Brush growth was optimized, and the effect of solvent polarity on polymerization kinetics was modeled. Our results confirm that these polyelectrolytic macroinitiators represent an attractive alternative to silane-based ATRP initiators for SIP from commercially relevant planar surfaces such as metal oxides.

Experimental Section

Materials. 2-Hydroxyethyl methacrylate (HEMA), 2-hydroxypropyl methacrylate (HPMA), and glycerol monomethacrylate (GMA) monomers were kindly donated by Cognis Performance Chemicals (Hythe, UK). The latter two monomers contain isomeric impurities: there is 8 mol % 1,3-dihydroxyisopropyl methacrylate in "GMA", and "HPMA" contains 25 mol % 2-hydroxyisopropyl methacrylate.⁴⁶ 2-(Diisopropylamino)ethyl methacrylate (DPA; Scientific Polymer Products) was passed through an "inhibitor-removing column DHR-4" (Scientific Polymer Products) before use. All other reagents were obtained from Aldrich or Fisher and were used as received. Silicon wafers ((100) orientation, boron-doped, 0–100 Ω·cm) were purchased from Compant Technology (Peter-

borough, UK). Deionized water was obtained using an Elga Elgastat Option 3 system. The dialysis tubing was 1000 MWCO Spectra/Por 6 regenerated cellulose (Spectrum Labs).

Poly(glycerol monomethacrylate) (PGMA) with a target degree of polymerization of 50 was prepared by ATRP as described previously.⁴⁶ ¹H NMR indicated a conversion of >99%, and GPC analysis of the copolymer precursor indicated an M_n of 12 400 and a M_w/M_n of 1.31 against poly(methyl methacrylate) (PMMA) standards. The cationic polyelectrolytic macroinitiator used in this work was prepared by statistical copolymerization of HEMA with 2-(dimethylamino)ethyl methacrylate (DMA) using ATRP as described previously.³ The statistical copolymer precursor comprised 80 mol % DMA and 20 mol % HEMA, and its target degree of polymerization was 100. ¹H NMR spectroscopy confirmed complete esterification of the hydroxyl groups using 2-bromoisobutyryl bromide and complete quaternization of the tertiary amine groups using methyl iodide. GPC analysis of the copolymer precursor indicated an M_n of 14 800 and a M_w/M_n of 1.25 against PMMA standards.

Characterization. AFM studies were conducted using a Nanoscope III microscope (Veeco) operating in tapping mode. Ellipsometry studies were conducted using a rotating analyzer ellipsometer (Gaertner Scientific) with a 633 nm laser at an angle of incidence of 70°, assuming a refractive index of 1.5 for the grafted polymer chains.^{42,47} ¹H NMR spectra were recorded in D₂O using a 250 MHz Bruker AC spectrometer. Static water contact angles were measured using a 2 μL drop, which was allowed to reach equilibrium for 10 min in a saturated atmosphere. Contact angles were determined from digital images using the DropSnake program.⁴⁸

Polyelectrolyte adsorption studies were conducted using an AnaLight Bio200 dual polarization interferometer (DPI) fitted with a 633 nm laser. AnaLight200 version 2.1.0 software was used for simultaneous data acquisition and analysis. Data were acquired at 10 Hz and averaged to give an output of one data point per second. Prior to measurement, the waveguide chip was calibrated using a 80:20 v/v ethanol/water mixture. All experiments were carried out in demineralized water at 20 °C using a Peltier system to control the temperature to within ±0.005 °C. The eluent flow rate was controlled using a Harvard Apparatus PHD2000 programmable syringe pump. Typical flow rates were 13.3 μL min⁻¹ for adsorption and 50 μL min⁻¹ for rinses.

Synthesis of Anionic Macroinitiator. The anionic macroinitiator was prepared from a near-monodisperse PGMA precursor in a two-step, one-pot reaction (see Scheme 1). 36% of the PGMA hydroxy groups were esterified with 2-bromoisobutyryl bromide (BIBB) before 72% of the remaining hydroxyl groups were esterified with excess 2-sulfobenzoic acid cyclic anhydride (SBA), giving a total degree of esterification of 82%. PGMA (2.00 g, target degree of polymerization = 50, M_n 12 400, M_w/M_n = 1.31, 25.0 mmol of hydroxy groups) and triethylamine (1.26 g, 12.5 mmol) were dissolved in 10 mL of anhydrous DMF under nitrogen. The stirred solution was cooled to 0 °C, and BIBB (2.88 g, 12.5 mmol) was added dropwise for the first-stage esterification. After warming to room temperature, this solution was stirred overnight. To this reaction solution was added 40 mL of DMF and triethylamine (3.79 g, 37.5 mmol) for the second-stage esterification. After cooling to 0 °C, SBA (6.90 g, 37.5 mmol) was added, and the mixture was stirred for 6 days at room temperature under a nitrogen atmosphere. The crude product was precipitated into 400 mL of rapidly stirred diethyl ether, collected by vacuum filtration, dissolved in 50 mL of water, and purified by dialysis against water for 5 days and then alternately against saturated sodium chloride and water for a further 4 days. The purified product was isolated by freeze-drying as a cream-colored powder (4.16 g, 64%) and characterized by ¹H NMR spectroscopy.

Macroinitiator Adsorption from Aqueous Solution. Silicon wafers were cleaned and rendered hydrophilic by first washing with acetone, 2-propanol, and water and then immersion for 15 min in a mixture of ammonia solution (14 mL, 35 wt %), hydrogen peroxide solution (14 mL, 30 wt %), and water (71 mL) at 70 °C.

Wafers were removed, rinsed thoroughly with water, and dried under a stream of air. For cationic macroinitiator adsorption, wafers were used directly. For anionic macroinitiator adsorption, wafers were then amine-functionalized by exposure to (3-aminopropyl)-triethoxysilane (APTES) vapor at 0.2 mbar for 30 min at room temperature and then annealed in air for 30 min at 110 °C. Both cationic and anionic macroinitiators were adsorbed onto wafer surfaces from 0.1 wt % aqueous copolymer solutions overnight at room temperature. Wafers were thoroughly rinsed with water and dried under a stream of air before use. Typical ellipsometric thicknesses were 11 Å for cationic macroinitiator layers and 12 Å for combined APTES and anionic macroinitiator layers under ambient conditions.

Surface Patterning by Microcontact Printing of Macroinitiator. Microcontact printing was conducted using a PDMS stamp fabricated by standard procedures. Following Krol et al.,⁴⁹ this stamp was “inked” by immersion in a 0.1 wt % aqueous solution of cationic macroinitiator for 15 min. The stamp was removed from solution, dried under a compressed air stream, and brought into conformal contact with a clean wafer surface. After 5 min, the stamp was removed, and the treated wafer was rinsed with water before polymerization.

Surface-Initiated ATRP. Surface-initiated polymerizations were conducted using HEMA, GMA, HPMA, DEA, and DPA in various solvents at room temperature. Specific details for a typical protocol are given below for HEMA in 1:1 v/v methanol/water.

HEMA, water, and methanol were separately degassed by nitrogen purging for 30 min. HEMA (10 mL, 10.7 g, 82.3 mmol), water (5 mL), and methanol (5 mL) were transferred by syringe into a flask, followed by Cu(I)Cl (138 mg, 1.39 mmol), Cu(II)Br₂ (90 mg, 0.404 mmol), and 2,2'-bipyridine (610 mg, 3.91 mmol); this mixture was stirred under a nitrogen purge to aid dissolution. Aliquots were transferred by syringe to Schlenk tubes (contained in a “Carousel 12 Reaction Station”, Radleys, UK) containing ca. 1 cm² pieces of macroinitiator-coated wafer under nitrogen. After various times, individual tubes were opened to the air and the polymer brush-coated wafers were removed. To remove the spent ATRP catalyst, each wafer was rinsed thoroughly with ca. 25 mL of water followed by ca. 25 mL of methanol and then dried under a stream of compressed air. The mean thickness of each polymer brush layer was then determined by ellipsometry under ambient conditions.

Simulation of the Kinetics of Surface ATRP. A computer simulation using numerical integration by the Euler method was used to model the PHEMA film growth. The evolution of the polymer radical concentration over 21 h was followed using 10⁹ time steps, assuming ideal ATRP kinetics and physically realistic rate constants. Full details have been previously reported by Bruening and co-workers⁵⁰ and are given in the Supporting Information.

Results and Discussion

Anionic Macroinitiator Synthesis and Adsorption. In previous work by Vo et al., an anionic macroinitiator was synthesized from PHEMA in a two-step synthesis.⁴⁴ After esterification of a minor fraction (either 19 or 27%) of hydroxyl groups with BIBB, the remaining hydroxyl groups were derivatized with excess SBA so as to introduce aromatic sulfonate groups and hence produce a “strong” anionic macroinitiator whose charge density is essentially independent of the solution pH.

For a given polymer molecular weight, thicker brushes are obtained at higher (macro)initiator grafting densities.⁵¹ Conversely, if the initiator surface density is too low, it is possible that the brush regime cannot be accessed and the grafted polymer chains may adopt a mushroom conformation.^{52,53} However, esterification of a higher fraction of hydroxyl groups on the PHEMA precursor with BIBB will necessarily lower the anionic charge density of the macroinitiator and potentially

Table 1. Adsorbed Amounts and Calculated Surface Densities of Bromoester Groups Determined by Dual Polarization Interferometry for the Cationic and Anionic Macroinitiators Electrostatically Adsorbed from Aqueous Solution at 20 °C onto Either Silicon Oxynitride or Aminated Silicon Oxynitride, Respectively

macroinitiator type	adsorbed mass/ mg m ⁻²	surface density of bromoester groups/nm ⁻²
cationic	0.86 ± 0.03	0.53 ± 0.02
anionic	1.03 ± 0.06	1.03 ± 0.06

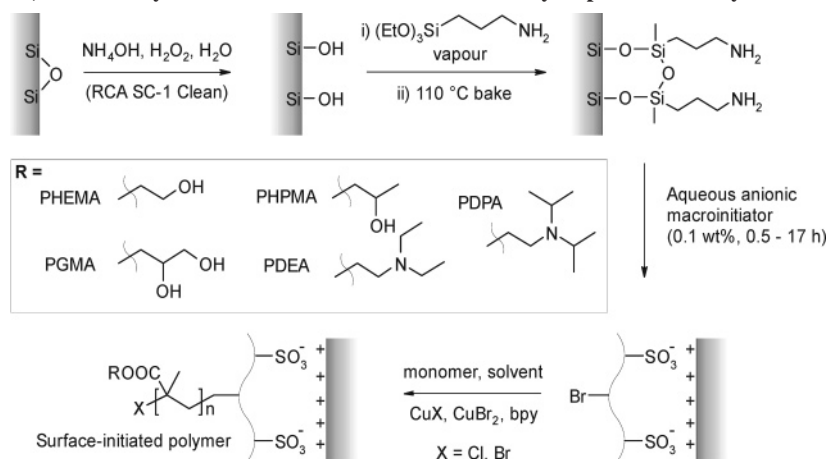
compromise its electrostatic adsorption to the surface. In view of this, PGMA was identified as a preferred precursor for the synthesis of anionic macroinitiators, since it contains two hydroxy groups per monomer repeat unit. This allows a relatively high surface density of bromoester initiator sites to be achieved while still retaining a relatively high charge density on the macroinitiator. Following Vo et al., a new anionic macroinitiator was synthesized from PGMA, with 36% of hydroxyl groups esterified with BIBB and 46% esterified with excess SBA as judged by ¹H NMR spectroscopy. This one-pot synthesis is shown in Scheme 1 and proved very convenient, with the final anionic macroinitiator being isolated with an overall yield of 64%.

DPI was used to determine the amount of macroinitiator electrostatically adsorbed onto planar surfaces from aqueous solution. The underlying theory of DPI and its application has been described in detail elsewhere.^{54–57} Only the basic principles are given here. Briefly, sensor chips consisting of two silicon oxynitride optical waveguides stacked on top of each other are illuminated with polarized laser light. Upon recombination, the light from the two waveguides interferes, producing Young's interference fringes which are captured by a CCD. The sensing waveguide is exposed to adsorbate, whereas the reference waveguide is not. As the evanescent field in the sensing waveguide interacts with the adsorbing layer, the speed of light within the waveguide is reduced with respect to the reference waveguide. This changes the phase difference between them and hence also the position of the interference fringes. This phase change can be directly related to the refractive index and absolute thickness of the adsorbed layer.

Classical optical theory does not distinguish between a diffuse thick layer and a compact thin layer of adsorbate. However, by illuminating the chip with two orthogonally polarized light beams, absolute refractive indices and thicknesses can be determined separately, since the two beams respond slightly differently to the adsorbed layer. DPI can be used to make measurements with very high thickness resolution (typically 0.01 nm). Unlike ellipsometry, which requires modeling of refractive indices, this relatively new technique measures the absolute refractive index and the layer thickness. Other parameters (e.g., adsorbed amounts) are then calculated from this information.

The adsorption of both the newly synthesized anionic macroinitiator and the previously reported cationic macroinitiator^{3,43} onto either silicon oxynitride or aminated silicon oxynitride (which are reasonably close analogues for oxidized silicon wafer or aminated silica, respectively) was measured.

The adsorbed amounts for both the cationic and anionic macroinitiators were examined after three 30 min periods of adsorption, with each adsorption period being followed with a water rinse. The two curves indicating the kinetics of adsorption of each macroinitiator are shown in the Supporting Information. Final adsorbed amounts and calculated surface densities of bromoester groups are shown in Table 1. The adsorbed amounts determined here for planar surfaces closely correspond to those previously reported for the electrostatic adsorption of macro-

Scheme 2. Electrostatic Adsorption of Anionic Macroinitiator onto Cationic Amine-Functionalized Silicon Wafers from Aqueous Solution, Followed by Surface-Initiated ATRP of Various Hydrophilic Methacrylic Monomers^a

^a Only the major isomers of PHPMA and PGMA are shown for clarity.

initiators onto particulate substrates ($0.6\text{--}0.9 \text{ mg m}^{-2}$ for cationic and 1.0 mg m^{-2} for anionic macroinitiators^{3,44}). Moreover, the greater bromoester content of the anionic macroinitiator leads to a significantly higher surface density of ATRP initiator sites. Since the polymer brush thickness is proportional to initiator surface density, this should lead to the growth of thicker brushes under otherwise identical conditions. This is indeed the case for PHEMA brushes (see later). As a comparison, bromoester density for a commonly used thiol initiator monolayer on gold is calculated to be around 5 nm^{-2} (assuming a close-packed monolayer)⁵⁸ although polymer chains that are in the brush regime can still be grown from gold at a density of 0.5 nm^{-2} from a monolayer diluted 10-fold with noninitiating thiol.⁵⁹ For silane initiators on silica nanoparticles, densities of $2\text{--}5 \text{ nm}^{-2}$ have been measured.⁶⁰

Surface-Initiated ATRP (SI-ATRP) from Electrostatically Adsorbed Anionic Macroinitiator. SI-ATRP was conducted by first preparing a solution of the methacrylic monomer in either water, alcohol, or the desired water/alcohol mixture, adding either Cu(I)Br or Cu(I)Cl catalyst, bpy ligand, and Cu(II)Br_2 , and transferring this solution so as to completely cover wafer pieces placed in individual Schlenk tubes (Scheme 2). Polymerizations were terminated by removing these wafers from solution, followed by thorough rinsing with solvent. No free initiator was added to the polymerization solution; i.e., the polymerization is surface-confined. Assuming reasonably good living character for the surface polymerization, the amount of free polymer formed in solution should be negligible. The addition of Cu(II)Br_2 ($\text{Cu(II)Br}_2/\text{Cu(I)X}$ molar ratio = 0.30) to the polymerizing solution was required because the relatively small number of propagating chains produces insufficient Cu(II) for good control.⁴⁷

The SI-ATRP of three hydroxy-functional methacrylates (HEMA, GMA, and HPMA) and two tertiary amine methacrylates (DEA and DPA) was examined in this study. It is essential to optimize the rate of polymerization to obtain thick polymer brushes by SIP: rapid polymerizations with a high initial growth rate usually terminate at relatively low brush thicknesses due to a relatively high polymer radical concentration,⁵⁰ whereas very slow polymerizations are often susceptible to various side-reactions (such as disproportionation of copper(I) species) that eventually terminate the growing chains before sufficiently thick films can be produced.⁶¹ In this context, it is worth recalling that the rate of termination is proportional to the square of the

polymer radical concentration $[\text{P}^\bullet]$, whereas the rate of propagation is simply proportional to $[\text{P}^\bullet]$.

In view of the extensive literature reported for the surface polymerization of HEMA in methanol/water mixtures,^{3,47,62,63} it was decided to focus on this “model” monomer in order to examine the effect of varying the rate of polymerization on the brush growth and final brush thickness. We and others have previously reported that the presence of water greatly accelerates the rate of ATRP of HEMA (and other methacrylic monomers), albeit at the expense of control.^{64–67} Hence systematic variation of the water content of the polymerizing mixture allows optimization of the conditions required for producing thick PHEMA films.

Following earlier work by Bruening and co-workers, the SI-ATRP of HEMA was conducted in water, a 1:1 v/v methanol/water mixture, and methanol using a $\text{Cu(I)Cl}/\text{Cu(II)Br}_2$ catalyst/deactivator system⁴⁷ from anionic macroinitiator adsorbed onto an aminated silicon wafer. Periodic removal of wafers from polymerizing solutions at various times followed by ellipsometric measurement of the brush thicknesses allowed convenient monitoring of the polymerization kinetics (Figure 1a).

Variation of the polymerization medium had a dramatic effect on the initial growth rate: polymerizations conducted in a 1:1 methanol:water mixture and pure water had a much greater initial rate than that conducted in methanol, as expected. It is also clear that there is an optimum polymerization medium for achieving thick films. Using methanol, the growth rate is reasonably constant (as would be expected from well-controlled SIP in the brush regime⁵¹), but at 20°C the brushes grow too slowly to be of practical use. Aqueous polymerizations are initially the fastest but suffer from substantial termination: it is difficult to achieve brush thicknesses greater than 20 nm. However, a reasonable compromise between control and polymerization rate was achieved using a 1:1 v/v methanol/water mixture. This solvent composition allows relatively thick PHEMA layers of up to 33 nm to be grown within 21 h. It should be noted that near-linear growth kinetics and films of these thicknesses can only be achieved if the tethered chains are in the brush regime,^{51,53} which confirms the high initiator density and initiator efficiency of our “second-generation” anionic macroinitiator.

The general form of these growth curves can be predicted by modeling the evolution of polymer radical concentration with time, assuming ideal ATRP kinetics. Following the work of Kim

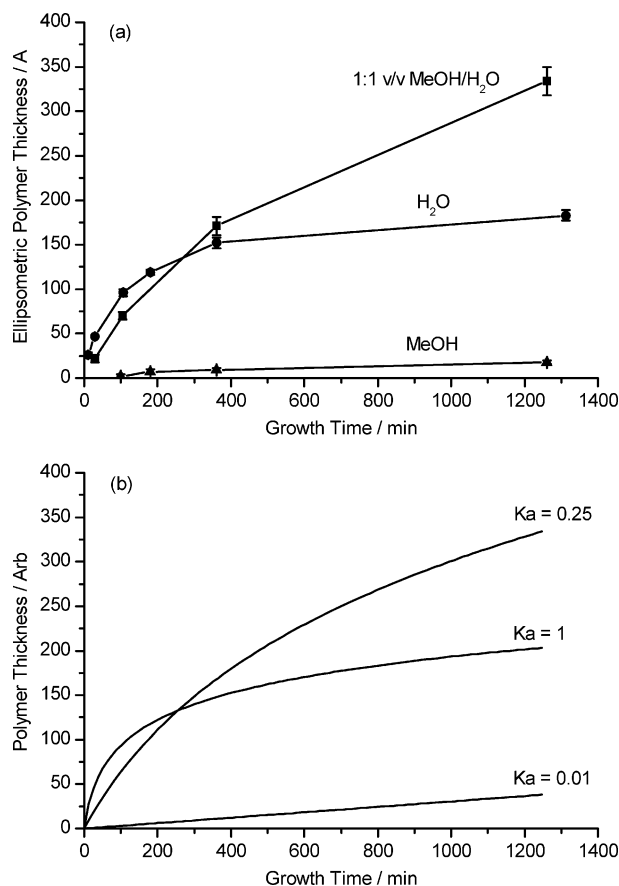


Figure 1. (a) Evolution of ellipsometric brush thickness with growth time for the surface ATRP of HEMA from anionic macroinitiator on aminated silicon wafers using water (●), 1:1 v/v methanol/water (■), and methanol (▲) as the solvent and a CuCl/CuBr₂ catalyst. The HEMA concentration was 4.12 M, and the HEMA:CuCl:CuBr₂:bpy molar ratio was 60:1:0.3:2.8. All polymerizations were conducted at 20 °C. (b) Numerical simulations of PHEMA brush growth assuming $k_a = 1$, 0.25, and 0.01 L mol⁻¹ s⁻¹. Reagent concentrations were the same as those used in the polymerizations: k_d and k_t were equal to 1×10^6 L mol⁻¹ s⁻¹ and 1×10^8 L mol⁻¹ s⁻¹, respectively.

et al.,⁵⁰ a simple computer program was written in C in which the effect of the following three reactions on the polymer radical concentration was considered: activation of dormant polymer chains by Cu(I) species, deactivation of polymer radicals by Cu(II) species, and bimolecular termination. Since a negligible amount of polymer is grown in a surface-confined polymerization (i.e., the conversion is close to zero), then to a first approximation the monomer concentration remains constant. Assuming that the concentrations of Cu(I) and Cu(II) are also constant, it can be shown that the rate of polymerization is simply a linear function of the polymer radical concentration. Also, for polymer chains in the brush regime, the film thickness is proportional to the degree of polymerization.⁵¹ This allows the evolution of brush thickness with time to be modeled by simply taking a cumulative sum of the polymer radical concentration at each time interval in the computer simulation. Full details of this simulation can be found in the Supporting Information.

Changing the solvent polarity affects the structure of the ATRP catalyst^{61,68} as well as the relative rates of activation,⁶⁹ deactivation,⁶¹ and termination.⁷⁰ However, in this simple model it is assumed that the only effect of increasing the water content of the polymerizing solution is to increase the activation rate constant k_a .⁶⁹ By choosing reasonable values for the deactivation and termination rate constants, e.g., $k_d = 1 \times 10^6$ L mol⁻¹ s⁻¹

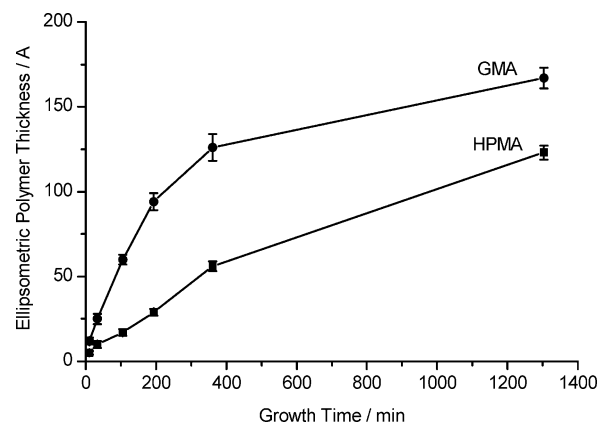


Figure 2. Ellipsometric thickness against growth time for surface-initiated polymerization of HPMA (■) and GMA (●) from anionic macroinitiator on aminated silicon wafers using a 1:1 v/v methanol/water solvent mixture and a CuCl/CuBr₂ catalyst. Monomer concentrations were [HPMA] = 3.60 M and [GMA] = 3.34 M. The monomer:CuCl:CuBr₂:bpy molar ratio was 60:1:0.3:2.8 in each case. Both polymerizations were conducted at 20 °C.



Figure 3. Static water contact angles determined at 20 °C for three hydroxyl-functional brushes: PHPMA (12 nm thickness), PHEMA (17 nm thickness), and PGMA (13 nm thickness).

and $k_t = 1 \times 10^8$ L mol⁻¹ s⁻¹,^{30,50} the essential features of the PHEMA growth data could be reproduced using just three values of k_a : 1.00, 0.25, and 0.01 L mol⁻¹ s⁻¹ (Figure 1b).

Since using the Cu(I)Cl/Cu(II)Br₂ catalyst in a 1:1 methanol/water mixture gave thick PHEMA brushes, these conditions were also employed for the surface ATRP of two other hydroxyl-functional methacrylic monomers, namely PGMA and PHPMA. PGMA contains two hydroxyl groups per monomer repeat unit and is therefore highly hydrophilic: this may be particularly useful for the postfunctionalization and cross-linking of polymer brushes. PHPMA exhibits temperature-dependent water solubility⁷¹ and may allow the fabrication of thermoresponsive surfaces. Brush thicknesses of 12 and 17 nm thickness were achieved for PHPMA and PGMA, respectively, within 21 h at 20 °C under identical conditions (Figure 2).

These three hydroxyl-functional methacrylic monomers provide an interesting series of increasing hydrophilic character: HPMA monomer is water-soluble up to 13% at 20 °C but PHPMA is water-insoluble,⁷¹ HEMA is water-miscible in all proportions while PHEMA is generally considered to be water-swallowable (but actually exhibits molecular weight-dependent water solubility at lower degrees of polymerization⁶⁶) and both GMA and PGMA are fully water-soluble.⁴⁶ The expected trend of increasing hydrophilic character (PHPMA < PHEMA < PGMA) was observed for the static contact angles determined for water droplets placed on these three polymer brushes (Figure 3).

Poly(tertiary amine methacrylates) typically exhibit pH-dependent solubility⁷² and can be used to produce pH-responsive surfaces.^{11,12,15} For example, PDEA has a pK_a of 7.3 and is insoluble above this pH. Following the same methodology as that used for the PHEMA brush growth described above, PDEA films were grown in various methanol/water mixtures, with Cu(I)Cl being replaced by Cu(I)Br, and the brush growth kinetics were studied (Figure 4).

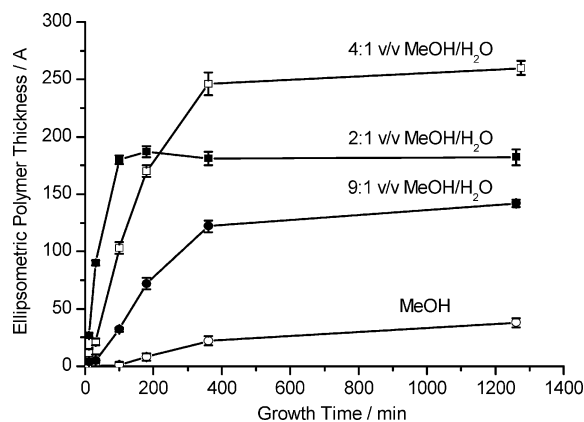


Figure 4. Ellipsometric brush thickness against time for the surface ATRP of 2-(diethylamino)ethyl methacrylate (DEA) from anionic macroinitiator on aminated silicon wafers using 2:1 v/v methanol/water (■), 4:1 v/v methanol/water (□), 9:1 v/v methanol/water (●), and methanol (○) as the solvent and a CuBr/CuBr₂ catalyst. The monomer concentration was 2.59 M (2.09 M for the polymerization in 2:1 v/v methanol/water) and the DEA:CuBr:CuBr₂:bpy molar ratio was 60:1:0.3:2.8. All polymerizations were conducted at 20 °C.

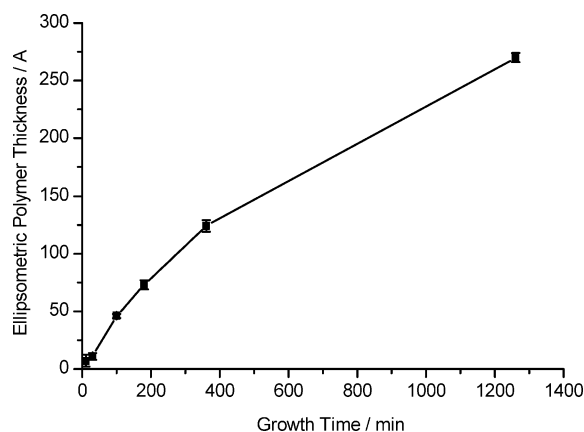


Figure 5. Ellipsometric thickness against growth time for surface-initiated polymerization of 2-(diisopropylamino)ethyl methacrylate (DPA) from anionic macroinitiator on aminated silicon wafers using a 95:5 v/v propan-2-ol/water solvent mixture and a CuCl catalyst. The DPA concentration was 2.24 M, and the DPA:CuCl:CuBr₂:bpy molar ratio was 60:1:0.3:2.8. The polymerization was conducted at 20 °C.

As observed for the HEMA surface polymerizations, increasing the water content increases the initial rate of polymerization. Again, the solvent mixture with the highest water content (2:1 v/v methanol/water) produces the fastest initial growth but suffers the greatest degree of termination and hence ultimately does not produce thick brush layers. The thickest PDEA brush layers were obtained using 4:1 v/v methanol/water as the solvent, with 26 nm brushes being grown within 21 h. Termination appears to be more prevalent for DEA compared to HEMA under the same conditions. This may be due to nucleophilic attack of terminal Br groups on growing chains by side-chain tertiary amines.⁷³

PDPA homopolymer has a pK_a of 6.3,⁷⁴ which is lower than that of PDEA; it may also prove useful for producing pH-responsive brushes. Following work by McDonald and Rannard,⁶⁷ a 95:5 propan-2-ol/water solvent mixture and Cu(I)Cl catalyst were selected for DPA polymerization at 20 °C. However, no Cu(II) was added to this polymerization because the Cu(II)Br₂/2bpy complex has poor solubility under these conditions. Even in the absence of this deactivator, the polymerization appeared reasonably controlled, with PDPA brush thicknesses of up to 27 nm being achieved within 21 h (Figure 5).

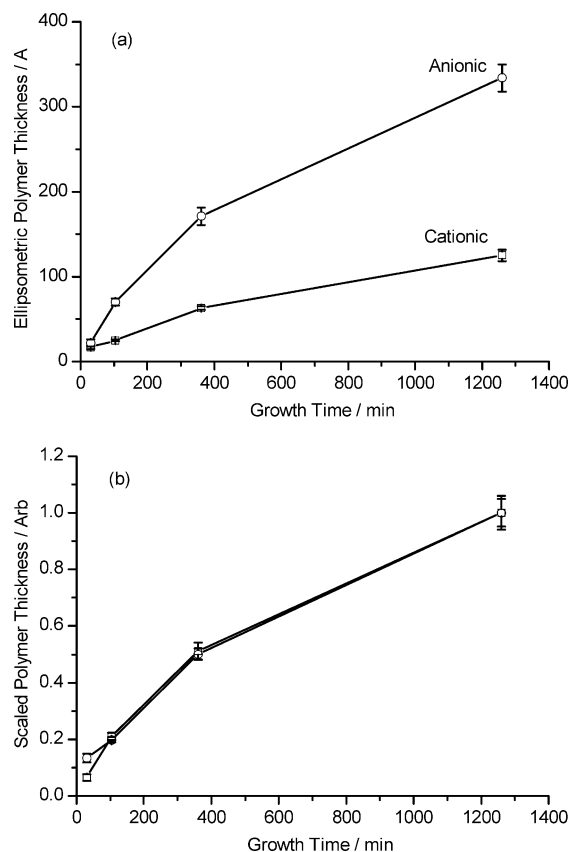


Figure 6. (a) Ellipsometric brush thickness against growth time for surface-initiated polymerization of HEMA at 20 °C using a 1:1 v/v methanol/water solvent mixture from anionic (○) and cationic (□) macroinitiators under otherwise identical conditions. Monomer concentration was 4.12 M, and the monomer:CuCl:CuBr₂:bpy molar ratio was 60:1:0.3:2.8. Both polymerizations were conducted at 20 °C. (b) These same growth curves normalized with respect to brush thickness after 21 h.

Direct Comparison of Anionic and Cationic Macroinitiators. Although polyelectrolytic macroinitiators previously developed by our group have been used for SIP from various colloidal sols,^{3,43,44} there are no prior literature reports describing the use of such macroinitiators for SIP from planar surfaces. Thus, it was decided to evaluate our original cationic macroinitiator adsorbed onto anionic silica wafer surfaces and compare its performance with the new anionic macroinitiator adsorbed onto cationic surfaces described above. Physical adsorption of a cationic macroinitiator onto cleaned silicon wafers from a 0.1 wt % aqueous solution for 20 h allowed the subsequent growth of PHEMA brushes at 20 °C using a 1:1 v/v methanol/water solvent mixture (see Figure 6a).

Clearly, PHEMA brushes grown from the anionic macroinitiator are considerably thicker than those grown from the cationic macroinitiator under the same conditions. Normalizing these growth curves with respect to the brush thickness attained after 21 h confirms very similar polymerization kinetics (see Figure 6b). Since the monomer concentration, temperature, catalyst concentration, etc., are all held constant, the thicker brushes produced using the anionic macroinitiator are simply due to the higher surface density of bromoester initiator sites, as expected on the basis of DPI data.

Surface Patterning by Microcontact Printing. Surface-initiated polymerization is often used in combination with microcontact printing⁷⁵ to produce topographically patterned planar surfaces. By printing initiator directly (or by printing a noninitiating molecule and then "backfilling" with initiator) the growth of polymer brushes can be restricted only to areas

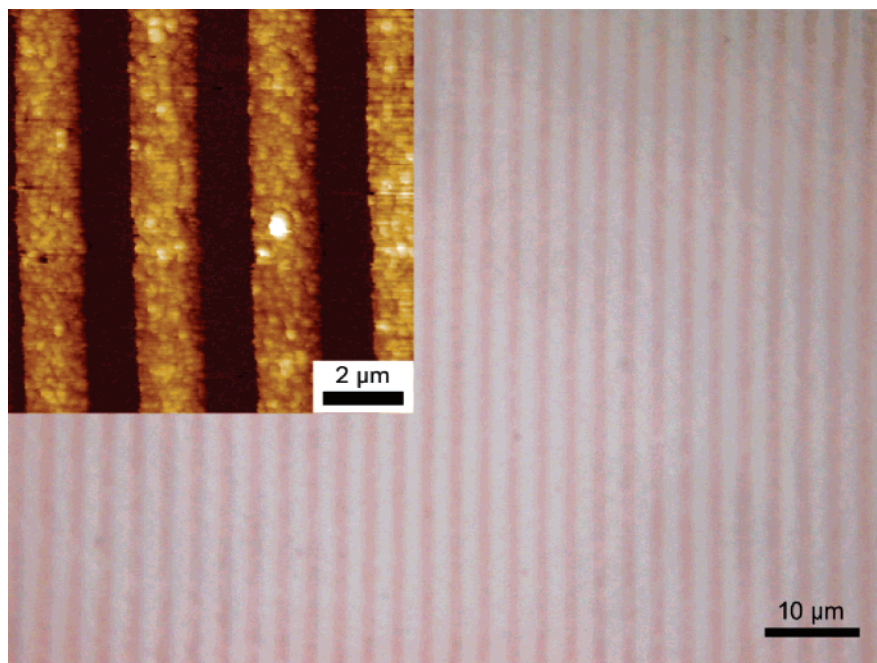


Figure 7. Optical microscope image showing micropatterned surface-initiated PHEMA brushes grown using microcontact-printed cationic macroinitiator layers adsorbed onto a cleaned silicon wafer. Inset: tapping-mode AFM image of these PHEMA brushes (z -scale 150 nm, feature height is ca. 54 nm).

defined by the stamp pattern. The majority of this work has been carried out with thiol-based ATRP initiators on gold surfaces^{62,76,77} although some work has also been reported for silanes on silica.^{78,79} Although most microcontact printing has been conducted with small molecule “ink”, printing of polyelectrolytes is not unknown.^{49,80} To further demonstrate that the polyelectrolytic macroinitiators reported in this work are a realistic replacement for silanes on planar metal oxide surfaces, we examined the feasibility of microcontact printing the cationic macroinitiator onto silicon wafers using a micropatterned PDMS stamp. PHEMA brushes were then grown for 21 h using a 1:1 v/v methanol/water solvent mixture under the conditions described above to produce topographically well-defined micrometer-sized PHEMA stripes. Optical microscopy studies confirmed the uniformity of these features over a wide surface area and AFM studies indicated a mean brush height of ~ 54 nm (see Figure 7). We note that this thickness is significantly greater than that achieved using cationic macroinitiator electrostatically adsorbed from aqueous solution. This is not unexpected, since it has been shown that microcontact printing of polyelectrolytes transfers a thicker layer than adsorption from solution,⁸⁰ thus producing a higher initiator density and hence thicker brushes.

Conclusions

Surface ATRP has been demonstrated for the first time for polyelectrolytic macroinitiators adsorbed onto planar substrates. Electrostatic adsorption of macroinitiators was determined using dual polarization interferometry, which enables the absolute values of both the layer thickness and the refractive index to be directly and unambiguously determined. A new “second-generation” anionic macroinitiator containing a relatively high proportion of bromoester initiator sites produced significantly higher grafting densities than the previously reported cationic macroinitiator. Although the surface concentrations of initiator sites for these macroinitiators are less than that reported for a typical thiol monolayer, they are nevertheless sufficient to access

the brush regime, allowing metal oxide surfaces to be used for surface ATRP without the need for silane synthesis.

The efficient growth of both PHEMA and PDEA brushes from anionic macroinitiator-coated surfaces was demonstrated up to 33 and 26 nm, respectively. The effect of solvent composition on surface polymerization was investigated, and in addition, a computer simulation was used to model the ATRP kinetics. PHPMA and PGMA brushes were also grown up to 12 and 17 nm, respectively. The static water contact angle θ for water droplets for these three hydroxy-functional brushes were in the order PGMA < PHEMA < PHPMA, as expected. The successful growth of PDPA and PDEA brushes is expected to allow the production of pH-responsive surfaces with effective pK_a values that depend on both the brush density and the brush thickness. Patterning of polyelectrolytic macroinitiators by microcontact printing was also demonstrated, suggesting that this approach is both attractive and convenient for surface functionalization of commercially relevant surfaces such as silica, mica, and metal oxides. The application of these polyelectrolytic macroinitiators for the production of a wide range of functional polymer brushes on various substrates is currently under investigation.

Acknowledgment. EPSRC is acknowledged for two post-doctoral grants: GR/S60419 (C.-D.V.) and Platform grant GR/S25845/01 (S.E.). S.P.A. is the recipient of a five-year Royal Society/Wolfson Research Merit award. Claire Wilshaw and Prof. A. J. Ryan are thanked for use of a PDMS stamp for surface patterning. Unilever Research is thanked for permission to publish this work.

Supporting Information Available: DPI curves for the electrostatic adsorption of the anionic and cationic macroinitiators onto planar cationic and anionic substrates, respectively; details of the ATRP kinetics modeling studies. This material is available free of charge via the Internet at <http://pubs.acs.org>.

References and Notes

- (1) Milner, S. T. *Science* **1991**, *251*, 905.

- (2) Radhakrishnan, B.; Ranjan, R.; Brittain, W. J. *Soft Matter* **2006**, *2*, 386.
- (3) Chen, X. Y.; Armes, S. P.; Greaves, S. J.; Watts, J. F. *Langmuir* **2004**, *20*, 587.
- (4) Perruchot, C.; Khan, M. A.; Kamitsi, A.; Armes, S. P.; von Werne, T.; Patten, T. E. *Langmuir* **2001**, *17*, 4479.
- (5) Chen, X.; Randall, D. P.; Perruchot, C.; Watts, J. F.; Patten, T. E.; von Werne, T.; Armes, S. P. *J. Colloid Interface Sci.* **2003**, *257*, 56.
- (6) Corbierre, M. K.; Cameron, N. S.; Sutton, M.; Mochrie, S. G. J.; Lurio, L. B.; Ruhm, A.; Lennox, R. B. *J. Am. Chem. Soc.* **2001**, *123*, 10411.
- (7) Ohno, K.; Morinaga, T.; Koh, K.; Tsujii, Y.; Fukuda, T. *Macromolecules* **2005**, *38*, 2137.
- (8) Sun, L.; Baker, G. L.; Bruening, M. L. *Macromolecules* **2005**, *38*, 2307.
- (9) Sun, L.; Dai, J.; Baker, G. L.; Bruening, M. L. *Chem. Mater.* **2006**, *18*, 4033.
- (10) R  he, J.; Ballauff, M.; Biesalski, M.; Dziezok, P.; Gr  hn, F.; Johannsmann, D.; Houbenov, N.; Hugenberg, N.; Konradi, R.; Minko, S.; Motornov, M.; Netz, R. R.; Schmidt, M.; Seidel, C.; Stamm, M.; Stephan, T.; Usov, D.; Zhang, H. *Adv. Polym. Sci.* **2004**, *165*, 79.
- (11) Ayres, N.; Boyes, S. G.; Brittain, W. J. *Langmuir* **2007**, *23*, 182.
- (12) Geoghegan, M.; Ruiz-Perez, L.; Dang, C. C.; Parnell, A. J.; Martin, S. J.; Howse, J. R.; Jones, R. A. L.; Golestanian, R.; Topham, P. D.; Crook, C. J.; Ryan, A. J.; Sivia, D. S.; Webster, J. R. P.; Menelle, A. *Soft Matter* **2006**, *2*, 1076.
- (13) LeMieux, M. C.; Peleshanko, S.; Anderson, K. D.; Tsukruk, V. V. *Langmuir* **2007**, *23*, 265.
- (14) Moya, S.; Azzaroni, O.; Farhan, T.; Osborne, V. L.; Huck, W. T. S. *Angew. Chem., Int. Ed.* **2005**, *44*, 4578.
- (15) Sakai, K.; Smith, E. G.; Webber, G. B.; Baker, M.; Wanless, E. J.; B  t  n, V.; Armes, S. P.; Biggs, S. *Langmuir* **2006**, *22*, 8435.
- (16) Bumbu, G. G.; Wolkenhauer, M.; Kircher, G.; Gutmann, J. S.; Berger, R. *Langmuir* **2007**, *23*, 2203.
- (17) Zhou, F.; Shu, W.; Welland, M. E.; Huck, W. T. S. *J. Am. Chem. Soc.* **2006**, *128*, 5326.
- (18) Tugulu, S.; Arnold, A.; Sielaff, I.; Johnsson, K.; Klok, H. A. *Biomacromolecules* **2005**, *6*, 1602.
- (19) Ryan, A. J.; Crook, C. J.; Howse, J. R.; Topham, P.; Jones, R. A. L.; Geoghegan, M.; Parnell, A. J.; Ruiz-P  rez, L.; Martin, S. J.; Cadby, A.; Menelle, A.; Webster, J. R. P.; Gleeson, A. J.; Bras, W. *Faraday Discuss.* **2005**, *128*, 55.
- (20) Kobayashi, M.; Terayama, Y.; Hosaka, N.; Kaido, M.; Suzuki, A.; Yamada, N.; Torikai, N.; Ishihara, K.; Takahara, A. *Soft Matter*, in press.
- (21) Raviv, U.; Giasson, S.; Kampf, N.; Gohy, J.-F.; Jerome, R.; Klein, J. *Nature (London)* **2003**, *425*, 163.
- (22) Ramstedt, M.; Cheng, N.; Azzaroni, O.; Mossialos, D.; Mathieu, H. J.; Huck, W. T. S. *Langmuir* **2007**, *23*, 3314.
- (23) Mei, Y.; Elliott, J. T.; Smith, J. R.; Langenbach, K. J.; Wu, T.; Xu, C.; Beers, K. L.; Amis, E. J.; Henderson, L. J. *Biomed. Mater. Res.* **2006**, *79A*, 974.
- (24) Comrie, J. E.; Huck, W. T. S. *Langmuir* **2007**, *23*, 1569.
- (25) Edmondson, S.; Huck, W. T. S. *Adv. Mater.* **2004**, *16*, 1327.
- (26) Bhat, R. R.; Genzer, J.; Chaney, B. N.; Sugg, H. W.; Liebmann-Vinson, A. *Nanotechnology* **2003**, *14*, 1145.
- (27) Santer, S.; R  he, J. *Polymer* **2004**, *45*, 8279.
- (28) Kato, M.; Kamigaito, M.; Sawamoto, M.; Higashimura, T. *Macromolecules* **1995**, *28*, 1721.
- (29) Wang, J.-S.; Matyjaszewski, K. *J. Am. Chem. Soc.* **1995**, *117*, 5614.
- (30) Matyjaszewski, K.; Xia, J. *Chem. Rev.* **2001**, *101*, 2921.
- (31) Edmondson, S.; Osborne, V. L.; Huck, W. T. S. *Chem. Soc. Rev.* **2004**, *33*, 14.
- (32) Ma, H.; Wells, M.; Beebe, T. P., Jr.; Chilkoti, A. *Adv. Funct. Mater.* **2006**, *16*, 640.
- (33) Zhou, F.; Hu, H.; Yu, B.; Osborne, V. L.; Huck, W. T. S.; Liu, W. *Anal. Chem.* **2007**, *79*, 176.
- (34) Husseman, M.; Malmstrom, E. E.; McNamara, M.; Mate, M.; Mecerreyes, D.; Benoit, D. G.; Hedrick, J. L.; Mansky, P.; Huang, E.; Russell, T. P.; Hawker, C. J. *Macromolecules* **1999**, *32*, 1424.
- (35) Wang, Y.; Hu, S.; Brittain, W. J. *Macromolecules* **2006**, *39*, 5675.
- (36) Brown, A. A.; Khan, N. S.; Steinbock, L.; Huck, W. T. S. *Eur. Polym. J.* **2005**, *41*, 1757.
- (37) Li, Y.; Tang, Y.; Narain, R.; Lewis, A. L.; Armes, S. P. *Langmuir* **2005**, *21*, 9946.
- (38) Limer, A.; Haddleton, D. M. *Macromolecules* **2006**, *39*, 1353.
- (39) Teodorescu, M.; Matyjaszewski, K. *Macromolecules* **1999**, *32*, 4826.
- (40) The synthesis of ester-based initiators is rendered problematic by the relative instability of hydroxy-functional alkoxy-silanes and chlorosilanes (due to self-condensation). Amine-functional alkoxy-silanes are available, and so in-situ synthesis of amide initiators is possible by reaction with 2-bromoisobutyl bromide.
- (41) St  hr, T.; R  he, J. *Macromolecules* **2000**, *33*, 4501.
- (42) Liu, Y.; Klep, V.; Zdyrko, B.; Luzinov, I. *Langmuir* **2004**, *20*, 6710.
- (43) Chen, X.; Armes, S. P. *Adv. Mater.* **2003**, *15*, 1558.
- (44) Vo, C. D.; Schmid, A.; Armes, S. P.; Sakai, K.; Biggs, S. *Langmuir* **2007**, *23*, 408.
- (45) Fulghum, T. M.; Patton, D. L.; Advincula, R. C. *Langmuir* **2006**, *22*, 8397.
- (46) Save, M.; Weaver, J. V. M.; Armes, S. P.; McKenna, P. *Macromolecules* **2002**, *35*, 1152.
- (47) Huang, W.; Kim, J. B.; Bruening, M. L.; Baker, G. L. *Macromolecules* **2002**, *35*, 1175.
- (48) Stalder, A. F.; Kulik, G.; Sage, D.; Barbieri, L.; Hoffmann, P. *Colloids Surf., A* **2006**, *286*, 92.
- (49) Krol, S.; Nolte, M.; Diaspro, A.; Mazza, D.; Magrassi, R.; Gliozzi, A.; Fery, A. *Langmuir* **2005**, *21*, 705.
- (50) Kim, J.-B.; Huang, W.; Miller, M. D.; Baker, G. L.; Bruening, M. L. *J. Polym. Sci., Part A: Polym. Chem.* **2003**, *41*, 386.
- (51) Tomlinson, M. R.; Genzer, J. *Macromolecules* **2003**, *36*, 3449.
- (52) Ionov, L.; Zdyrko, B.; Sidorenko, A.; Minko, S.; Klep, V.; Luzinov, I.; Stamm, M. *Macromol. Rapid Commun.* **2004**, *25*, 360.
- (53) Wu, T.; Efimenko, K.; Vlcek, P.; Subr, V.; Genzer, J. *Macromolecules* **2003**, *36*, 2448.
- (54) Cross, G. H.; Reeves, A.; Brand, S.; Swann, M. J.; Peel, L. L.; Freeman, N. J.; Lu, J. R. *J. Phys. D: Appl. Phys.* **2004**, *37*, 74.
- (55) Cross, G. H.; Reeves, A. A.; Brand, S.; Popplewell, J. F.; Peel, L. L.; Swann, M. J.; Freeman, N. J. *Biosens. Bioelectron.* **2003**, *19*, 383.
- (56) Cross, G. H.; Ren, Y.; Freeman, N. J. *J. Appl. Phys.* **1999**, *86*, 6483.
- (57) Swann, M. J.; Peel, L. L.; Carrington, S.; Freeman, N. J. *Anal. Biochem.* **2004**, *329*, 190.
- (58) Kim, J. B.; Bruening, M. L.; Baker, G. L. *J. Am. Chem. Soc.* **2000**, *122*, 7616.
- (59) Jones, D. M.; Brown, A. A.; Huck, W. T. S. *Langmuir* **2002**, *18*, 1265.
- (60) von Werne, T.; Patten, T. E. *J. Am. Chem. Soc.* **2001**, *123*, 7497.
- (61) Tsarevsky, N. V.; Pintauer, T.; Matyjaszewski, K. *Macromolecules* **2004**, *37*, 9768.
- (62) Jones, D. M.; Huck, W. T. S. *Adv. Mater.* **2001**, *13*, 1256.
- (63) Bhat, R. R.; Chaney, B. N.; Rowley, J.; Liebmann-Vinson, A.; Genzer, J. *Adv. Mater.* **2005**, *17*, 2802.
- (64) Ma, I. Y.; Lobb, E. J.; Billingham, N. C.; Armes, S. P.; Lewis, A. L.; Lloyd, A. W.; Salvage, J. *Macromolecules* **2002**, *35*, 9306.
- (65) Robinson, K. L.; Khan, M. A.; de PazBanez, M. V.; Wang, X. S.; Armes, S. P. *Macromolecules* **2001**, *34*, 3155.
- (66) Weaver, J. V. M.; Bannister, I.; Robinson, K. L.; Bories-Azeau, X.; Armes, S. P.; Smallridge, M.; McKenna, P. *Macromolecules* **2004**, *37*, 2395.
- (67) McDonald, S.; Rannard, S. P. *Macromolecules* **2001**, *34*, 8600.
- (68) Wang, X. S.; Armes, S. P. *Macromolecules* **2000**, *33*, 6640.
- (69) Nanda, A. K.; Matyjaszewski, K. *Macromolecules* **2003**, *36*, 599.
- (70) Alvarez, J.; Encinas, M. V.; Lissi, E. A. *Macromol. Chem. Phys.* **1999**, *200*, 2411.
- (71) Madsen, J.; Armes, S. P.; Lewis, A. L. *Macromolecules* **2006**, *39*, 7455.
- (72) B  t  n, V.; Armes, S. P.; Billingham, N. C. *Polymer* **2001**, *42*, 5993.
- (73) Zhang, X.; Matyjaszewski, K. *Macromolecules* **1999**, *32*, 1763.
- (74) Bories-Azeau, X.; Armes, S. P.; van den Haak, H. J. W. *Macromolecules* **2004**, *37*, 2348.
- (75) Xia, Y.; Whitesides, G. M. *Angew. Chem., Int. Ed.* **1998**, *37*, 550.
- (76) Shah, R. R.; Merceyes, D.; Husemann, M.; Rees, I.; Abbott, N. L.; Hawker, C. J.; Hedrick, J. L. *Macromolecules* **2000**, *33*, 597.
- (77) Zhou, F.; Zheng, Z.; Yu, B.; Liu, W.; Huck, W. T. S. *J. Am. Chem. Soc.* **2006**, *128*, 16253.
- (78) Hamelink, P. J.; Huck, W. T. S. *J. Mater. Chem.* **2005**, *15*, 381.
- (79) Whiting, G. L.; Snaith, H. J.; Khodabakhsh, S.; Andreasen, J. W.; Breiby, D. W.; Nielsen, M. M.; Greenham, N. C.; Friend, R. H.; Huck, W. T. S. *Nano Lett.* **2006**, *6*, 573.
- (80) Jiang, X.; Zheng, H.; Gourdin, S.; Hammond, P. T. *Langmuir* **2002**, *18*, 2607.

MA070876R